



ELSEVIER

Applied Numerical Mathematics 33 (2000) 3–21

APPLIED
NUMERICAL
MATHEMATICS

www.elsevier.nl/locate/apnum

Enhanced spectral viscosity approximations for conservation laws [☆]

Anne Gelb ^{a,1}, Eitan Tadmor ^{b,*}^a Department of Mathematics, Arizona State University, Tempe, AZ 85287, USA^b Department of Mathematics, UCLA, Los-Angeles, CA 90095, USA

Abstract

In this paper we construct, analyze and implement a new procedure for the spectral approximations of nonlinear conservation laws. It is well known that using spectral methods for nonlinear conservation laws will result in the formation of the Gibbs phenomenon once spontaneous shock discontinuities appear in the solution. These spurious oscillations will in turn lead to loss of resolution and render the standard spectral approximations unstable. The Spectral Viscosity (SV-) method (Tadmor, 1989) was developed to stabilize the spectral method by adding a spectrally small amount of high-frequencies diffusion carried out in the dual space. The resulting SV-approximation is stable without sacrificing spectral accuracy. The SV-method recovers a spectrally accurate approximation to the *projection* of the entropy solution; the exact projection, however, is at best a first order approximation to the exact solution as a result of the formation of the shock discontinuities. The issue of spectral *resolution* is addressed by post-processing the SV-solution to remove the spurious oscillations at the discontinuities, as well as increase the first-order— $O(1/N)$ accuracy away from the shock discontinuities. Successful post-processing methods have been developed to eliminate the Gibbs phenomenon and recover spectral accuracy for the SV-approximation. However, such reconstruction methods require a priori knowledge of the locations of the shock discontinuities. Therefore, the detection of these discontinuities is essential to obtain an overall spectrally accurate solution. To this end, we employ the recently constructed *enhanced edge detectors* based on appropriate concentration factors (Gelb and Tadmor, 1999). Once the edges of these discontinuities are identified, we can utilize a post-processing reconstruction method, and show that the post-processed SV-solution recovers the exact entropy solution with remarkably high-resolution. We apply our new numerical method, the Enhanced SV-method, to two numerical examples, the scalar periodic Burgers' equation and the one-dimensional system of Euler equations of gas dynamics. Both approximations exhibit high accuracy and resolution to the exact entropy solution. © 2000 IMACS. Published by Elsevier Science B.V. All rights reserved.

Keywords: Spectral-viscosity methods; Enhanced edge detection; Piecewise smoothness; Concentration factors

[☆] Research was supported in part by NSF Grant No. DMS97-06827 and ONR Grant No. N00014-1-J-1076.

* Corresponding author. E-mail: tadmor@math.ucla.edu

¹ E-mail: ag@math.la.asu.edu

1. Introduction

In this paper we are interested in recovering the solutions to the initial boundary value problems associated with the nonlinear conservation law,

$$\frac{\partial}{\partial t} u(x, t) + \frac{\partial}{\partial x} f(u(x, t)) = 0, \quad (x, t) \in [-1, 1] \times [0, \infty), \quad (1.1)$$

subject to prescribed initial values at time $t = 0$ and augmented with the necessary boundary conditions at $x = \pm 1$. Because of their success in obtaining highly accurate results for smooth linear problems, we would like to employ (pseudo-)spectral methods to (1.1). Unfortunately, applying (pseudo-)spectral methods to nonlinear conservation laws yields disastrous, unstable results when shock discontinuities are formed [24,25]. A series of papers written to address this problem [5,18,24,25,27, . . .] have resulted in the successful development of the spectral viscosity (SV-)method. The SV-method is based on high-frequencies dissipation which stabilizes the (otherwise unstable) pseudo-spectral method *without* sacrificing the underlying spectral accuracy. However, due to the presence of shocks in the underlying entropy solution, the SV-method retains only *formal* spectral accuracy. More specifically, the SV-solution approximates the *projection* of the exact solution, and it is the exact projection which experiences a loss of accuracy due to spurious Gibbs oscillations. Hence, the SV-solution must be post-processed in order to recover its content of better accuracy. Although high accuracy can be achieved away from the shock discontinuities using spectrally accurate filters, e.g., [11,18,19], the results of such post-processing in the neighborhoods of shocks still suffer from smearing effects and/or spurious Gibbs oscillations.

We therefore propose a new method in Section 5, the enhanced SV-method, which is a fully automated numerical method offering stability, high accuracy, and high resolution at the shock locations. There are three major ingredients in the enhanced SV-method:

1. The SV-method [18,24,25,27]. This step provides a *stable* spectral approximation of (1.1). The computed SV-solution, $u_N(x, T)$, retains enough information of the exact solution so that post-processing is required only at the final time step, $t = T$. The SV-method is reviewed in Section 2.
2. Enhanced Edge Detection [8,9]. This step identifies the locations and amplitudes of the edges—jump discontinuities, rarefactions tips . . . in the computed SV-solution, $u_N(x, T)$. Here we recover the *high resolution* of the approximation at the shock discontinuities—a critical step for effective post-processing discussed below. The procedure of edge detection is outlined in Section 3.
3. The Gegenbauer post-processing method [12]. We post-process the computed SV-solution at the final time, $u_N(x, T)$. Once the locations (and amplitudes) of the various edges are known, this (one-sided) post-processing enables us to recover the exact solution with high resolution *up to* the discontinuities. We summarize the idea in Section 4.

Numerical results for the enhanced SV-method for the scalar periodic inviscid Burgers' equation as well as the one-dimensional system for the Euler equations of gas dynamics are provided in Section 6.

2. The Spectral Viscosity (SV) method

As stated in the introduction, we will use the spectral viscosity (SV-) method to stabilize the nonlinear spectral approximation of (1.1). The SV-method was introduced in [24] for the Fourier spectral method and has been subsequently extended to multidimensional problems and was developed to include both Legendre and Chebyshev cases, e.g., [1,5,16–18,20,21,25,27]. The idea of the SV-method is to

add a spectrally accurate vanishing viscosity to augment the spectral approximation of the nonlinear conservation laws. The spectral viscosity, added only to the high wave numbers, is strong enough to stabilize the solution yet small enough to retain formal spectral accuracy.

2.1. The periodic case

We wish to solve the periodic conservation law

$$\frac{\partial}{\partial t} u(x, t) + \frac{\partial}{\partial x} f(u(x, t)) = 0, \quad u(x, 0) = u_0(x) \tag{2.1}$$

by employing the N -degree trigonometric polynomial,

$$u_N(x, t) = \sum_{k=-N}^N \widehat{u}_k(t) e^{ikx}, \tag{2.2}$$

to approximate the Fourier projection of the exact entropy solution, $S_N u$. Here $\widehat{u}_k(t)$ represent either spectral or pseudo-spectral coefficients.

In the classical spectral method, we start with $u_N(x, 0) = S_N u_0(x)$ and let $u_N(x, t)$ evolve according to the approximate equation

$$\frac{\partial}{\partial t} u_N + \frac{\partial}{\partial x} [S_N(f(u_N))] = 0. \tag{2.3}$$

As explained in [24,25], the convergence of u_N towards the entropy solution of (2.1) may fail, even with additional smoothing. Instead, in the SV-method, (2.3) is augmented with high frequencies viscosity regularization

$$\frac{\partial}{\partial t} u_N + \frac{\partial}{\partial x} [S_N(f(u_N))] = \varepsilon_N \sum_{m < |k| \leq N} (ik)^{2s} \widehat{Q}_k(t) \widehat{u}_k(t) e^{ikx}. \tag{2.4}$$

The spectral viscosity on the right involves the following three ingredients:

- The viscosity amplitude of order $\varepsilon_N \sim N^{1-2s}$. Here, s denote the order of the super-viscosity, related to vanishing diffusion of order $2s$. The choice of $s = 1$ refers to the usual second-order vanishing viscosity; $s > 1$ (introduced in [27]) is related to super-viscosity.
- The effective size of the *inviscid* spectrum, $m = m_N$,

$$m \equiv m_N \sim N^\theta, \quad \theta < \frac{2s - 1}{2s};$$

Thus, related to the usual second-order viscosity ($s = 1$) for example, one finds $\sim \sqrt{N}$ viscous-free modes. A larger choice of s yields a corresponding increase of the spectrally accurate viscous-free spectrum (consult (2.5) below).

- The SV smoothing factors, $\widehat{Q}_k(t)$, which are activated only on high wavenumbers, $|k| > m_N$, satisfying

$$1 - \left(\frac{m}{|k|} \right)^{(2s-1)/\theta} \leq \widehat{Q}_k(t) \leq 1, \quad |k| > m_N.$$

The SV-method can be viewed as a compromise between the stable viscosity approximation which is restricted to first order accuracy (corresponding to $\theta = 0$), and the spectrally accurate yet unstable spectral method (2.3) (corresponding to $\theta = 1$). The additional SV on the right of (2.4) is small enough to retain the *formal* spectral accuracy of the underlying spectral approximation, i.e., the following estimate holds:

$$\left\| \varepsilon_N \frac{\partial^s}{\partial x^s} \left[Q(x, t) * \frac{\partial^s u_N}{\partial x^s} \right] \right\|_{H^{-p}(x)} \leq \text{Const} \cdot N^{-\theta(p-2s)} \|u_N\|_{L^2(x)}, \quad \forall p > 2s. \quad (2.5)$$

At the same time, this SV is shown in [24,25,27] to be large enough so that it enforces a sufficient amount of entropy dissipation, and hence, by compensated compactness arguments, to prevent the unstable spurious Gibbs' oscillations.

2.2. The non-periodic case

In order to handle the boundary conditions, a weak formulation of the spectral viscosity regularization is required for the non-periodic case [18]. The corresponding SV-method in this context can be summarized as follows.

Suppose \mathbf{P}_N denotes the space of algebraic polynomials of degree $\leq N$, and let $(L_k)_{k \geq 0}$ denote (for example) the orthogonal family of Legendre polynomials. Also let $\{\xi_j\}_{j=0}^N$ denote the Legendre Gauss–Lobatto points with the corresponding discrete weights $\{\omega_j\}_{j=0}^N$. The unique \mathbf{P}_N -interpolant given by

$$\mathcal{I}_N(\phi)(x) = \sum_{k=0}^N \hat{\phi}_k L_k(x), \quad \mathcal{I}_N(\phi)(\xi_j) = \phi(\xi_j), \quad j = 0, \dots, N, \quad (2.6)$$

where $\hat{\phi}_k$ are the discrete Legendre coefficients, $\hat{\phi}_k = (\phi, L_k)_N / \|L_k\|_N^2$, associated with the corresponding Gauss–Lobatto quadrature weights, satisfying $(\phi, \psi)_N := \sum \phi(\xi_j) \psi(\xi_j) \omega_j$.

We seek a solution of the form $u_N(x, t) = \sum_{k=0}^N \hat{u}_k(t) L_k(x) \in \mathbf{P}_N$ to approximate (1.1). Specifically we are interested in implementing the Legendre SV-method as a discrete collocation method corresponding to the Gauss–Lobatto quadrature points $\{\xi_j\}_{j=0}^N$ and weight function $\{\omega_j\}_{j=0}^N$:

$$\begin{aligned} \frac{\partial}{\partial t} u_N(\xi_i, t) + \frac{\partial}{\partial x} \mathcal{I}_N f(u_N)(\xi_i, t) &= -\varepsilon_N \frac{\partial}{\partial x} Q \left(\frac{\partial}{\partial x} u_N \right) (\xi_i, t), \quad 1 \leq i \leq N-1, \\ \frac{\partial}{\partial t} u_N(+1, t) + \frac{\partial}{\partial x} \mathcal{I}_N f(u_N)(+1, t) &= -\varepsilon_N \frac{\partial}{\partial x} Q \left(\frac{\partial}{\partial x} u_N \right) (+1, t) - \frac{\varepsilon_N}{\omega_N} Q \left(\frac{\partial}{\partial x} u_N \right) (+1, t). \end{aligned} \quad (2.7)$$

Assuming that $x = +1$ is an outflow boundary, the second term on the right prevents the creation of an (outflow) boundary layer. This, together with the prescribed inflow boundary values (say, at $x = -1$), furnish a complete statement of the SV-method.

Here the spectral viscosity operator Q is defined by

$$Q\phi = \sum_{k=0}^N \hat{Q}_k \hat{\phi}_k L_k, \quad \forall \phi = \sum_{k=0}^{\infty} \hat{\phi}_k L_k. \quad (2.8)$$

As before, the SV operator in (2.8) leaves an increasing portion of the spectrum viscous-free— $\hat{Q}_k = 0$ for the first m_N modes (typically, we set $m_N \sim \sqrt{N}$), while introducing high-frequencies dissipation of order $\hat{Q}_k > 1 - (m_N/k)^4$ for $k \geq m_N$.

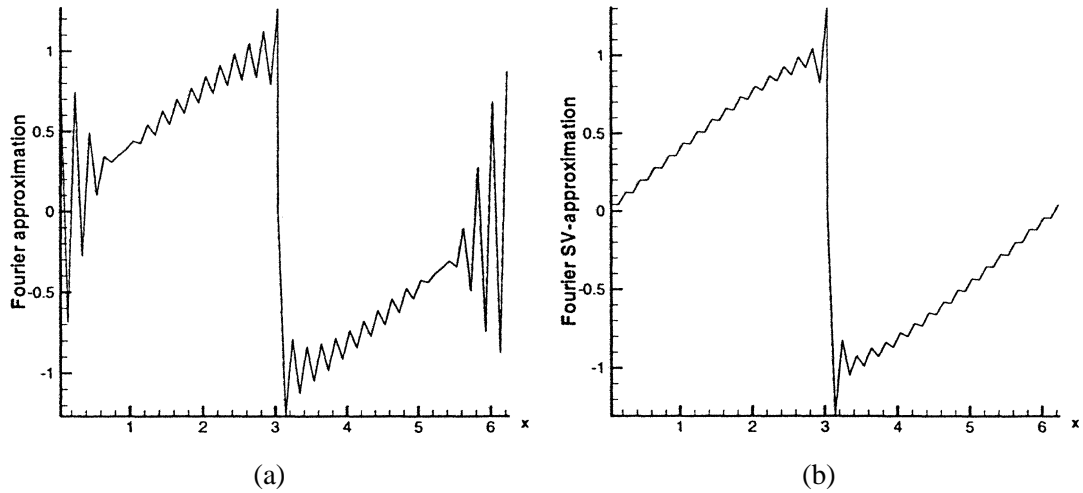


Fig. 1. The solution to the periodic inviscid Burgers' equation with periodic boundary conditions at time $T = 1$ using (a) the Fourier spectral approximation and (b) the Fourier SV-approximation for $N = 64$.

2.3. Numerical examples

To demonstrate the stability of the SV-method, we consider the inviscid Burgers' equation

$$\frac{\partial}{\partial t} u(x, t) + \frac{\partial}{\partial x} \left(\frac{u^2(x, t)}{2} \right) = 0, \tag{2.9}$$

in two different constructions:

1. *The periodic case* where $(x, t) \in [-\pi, \pi] \times [0, \infty)$, $u(x, 0) = \sin x$, and $u(-\pi, t) = g(t) = u(\pi, t)$.
2. *The non-periodic case* where $(x, t) \in [-1, 1] \times [0, \infty)$, $u(x, 0) = \frac{1}{2} \sin \pi x + 1$, and $u(-1, t) = g(t)$ (with $g(t) = u(1, t)$).

The results of the Fourier and Legendre SV-approximations are shown in Figs. 1 and 2.

It is indeed clear from Figs. 1 and 2 that the SV-method provides a stable approximation for the inviscid Burgers' equation. However, overall spectral accuracy cannot be realized at this stage since the underlying solution $u(x, T)$ contains shocks. Consequently, the *exact* projections, $S_N u(x, T)$ and $\mathcal{I}_N u(x, T)$ suffer from spurious Gibbs oscillations, which in turn are reflected in the SV solution depicted in Figs. 1 and 2.

In essence the problem is now reduced to reconstructing the piecewise smooth exact solution $f(x) := u(x, T)$, by extracting information from its approximate spectral projection, $S_N[f](x)$. The computed SV-solution is a highly accurate realization of the exact projection, i.e., $u_N(x, t) \sim S_N[f](x)$. It is well known that while $S_N[f](x)$ achieves spectral convergence for sufficiently smooth f 's, the accuracy is destroyed if f contains discontinuities, with the global accuracy deteriorating to first order and $O(1)$ Gibbs oscillations prevailing in the neighborhoods of the discontinuities. Therefore, a post-processing method must be applied to the final SV-approximation $S_N[f](x)$ for superior accuracy to be acquired. The mollifier proposed in [11] (in the periodic case) and in [18] (in the Legendre case), yield spectrally accurate results away from the discontinuities, but the results are smeared and/or oscillate over the shock discontinuities. This is for the solitary reason that the *edges* of $f(x)$ could not be computed

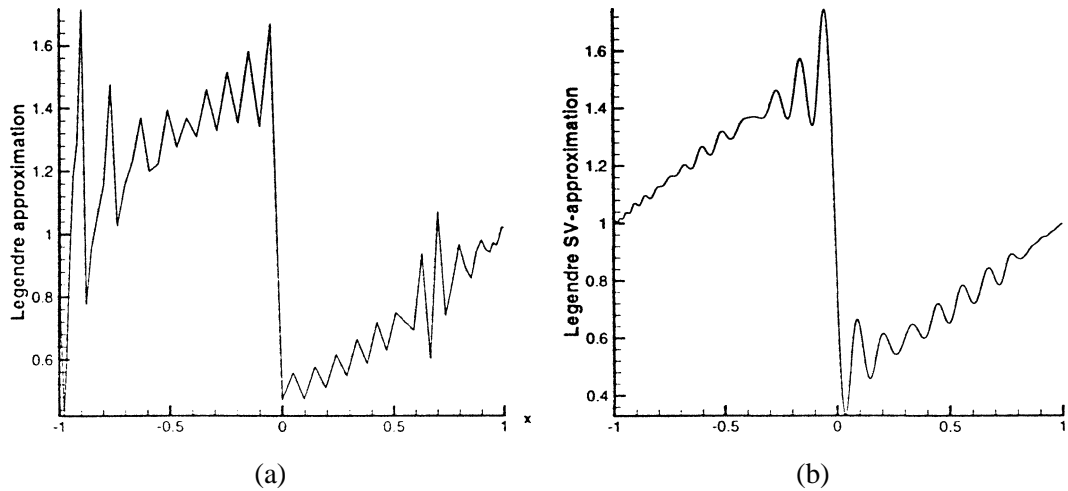


Fig. 2. The solution to the periodic inviscid Burgers' equation with periodic boundary conditions at time $T = 1.5$ using (a) the Legendre spectral approximation and (b) the Legendre SV-approximation for $N = 64$.

from the approximation $S_N[f](x)$. A spectrally accurate solution *up to* the discontinuities (i.e., without smearing/oscillations) critically depends upon accurately locating the edges of $f(x)$ from the information provided by $S_N[f](x)$. Such an edge detection method has been recently developed [8,9] and is reviewed in Section 3.

3. Detection of shock locations

Detection of edges is critical for the effective post-processing of $S_N[f](x)$, and hence for realizing the high-resolution content in the SV approximation of (1.1). Furthermore, accurate edge detection enables us to propose a fully automated approximation method (consult Section 5), broadening the scope of solvable nonlinear conservation laws. The enhanced version of the edge detection method introduced in [9] provides us with a simple way of finding the location and amplitude of one or more jump discontinuities of piecewise smooth f 's.

3.1. Concentration factors

The main idea of edge detection stems from the fact that the support of the conjugate Fourier partial sum $\tilde{S}_N[f](x) := \sum_{k=1}^N a_k \sin kx - b_k \cos kx$ approaches the singular support of $f(x)$ as $N \rightarrow \infty$ [3,30]. We refer to this as the *concentration* property. The approach, developed in [8], is based on the so-called 'concentration' factors $\sigma = \sigma(k/N)$ which are built into the conjugate Fourier sum, thus creating a generalized conjugate Fourier sum of the form

$$\tilde{S}_N^\sigma[f](x) = \sum_{k=1}^N \sigma\left(\frac{k}{N}\right) (a_k \sin kx - b_k \cos kx).$$

Admissible concentration factors $\sigma(k/N)$ accelerates the logarithmically slow concentration property of the conjugate Fourier partial sum $\tilde{S}_N[f](x)$, yielding faster convergence to the singular support of $f(x)$. This is the content of

Theorem 3.1 (Admissible concentration factors [8, Theorem 3.1]). *Let the concentration factors $\sigma(\cdot)$ be non-decreasing functions in $C^2[0, 1]$ satisfying*

$$\int_{1/N}^1 \frac{\sigma(x)}{x} dx \xrightarrow{N \rightarrow \infty} -\pi.$$

Then the generalized conjugate sum $\tilde{S}_N^\sigma[f]$ ‘concentrate’ near the jumps of f ,

$$\tilde{S}_N^\sigma[f](x) \xrightarrow{N \rightarrow \infty} [f](x), \quad [f](x) := f(x+) - f(x-),$$

with the convergence rate

$$|\tilde{S}_N^\sigma[f](x)| \leq \text{Const} \left(\frac{\log N}{N} + \left| \sigma \left(\frac{1}{N} \right) \right| \right) \tag{3.1}$$

for x ’s away from the jump discontinuities.

A similar procedure—involving concentration factors and conjugate sums, applies to discrete projections, $\mathcal{I}_N(f)$ —consult [8, Theorem 4.1].

3.2. Example of an admissible concentration factor

As an example, consider the family of concentration factors $\sigma^r(\xi) := -\pi r \xi^r$; for odd r ’s, this family of concentration factors amounts to differentiated Fourier partial sums:

$$\begin{aligned} \tilde{\mathcal{I}}_N^{\sigma^{2p+1}}[f](x) &= -\frac{\pi(2p+1)}{N^{2p+1}} \sum_{k=1}^N k^{2p+1} (a_k \sin kx - b_k \cos kx) \\ &= (-1)^p \frac{\pi(2p+1)}{N^{2p+1}} \frac{d^{2p+1}}{dx^{2p+1}} \mathcal{I}_N(f)(x), \end{aligned} \tag{3.2}$$

where the derivative of non-integer p is defined by the left-hand side of (3.2). The case $p = 0$ goes back to Fejer; consult [14] and the references therein. This leads to

$$(-1)^p \frac{\pi(2p+1)}{N^{2p+1}} \mathcal{I}_N^{(2p+1)}(f)(x) \rightarrow [f](x), \tag{3.3}$$

which enables the extension to the Legendre and Chebyshev (pseudo-)spectral methods (with the proper weight function and scaling variables) [9].

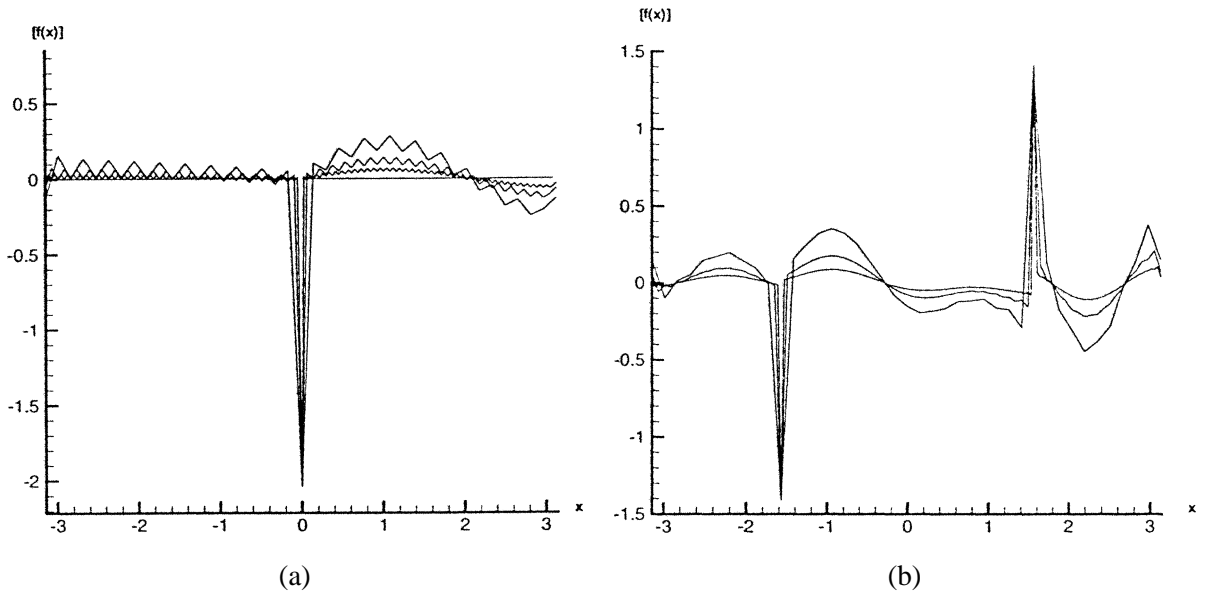


Fig. 3. Detection of discontinuous edges of $f_a(x)$ (a) and $f_b(x)$ (b) using the concentration method based on the generalized conjugate Fourier partial sum $\tilde{S}_N^\sigma[f](x)$ with $p = 0$ in (3.2) for $N = 20, 40$ and 80 modes.

3.3. Numerical examples of the concentration method

To illustrate the concentration method, we consider the following two examples on $[-\pi, \pi]$:

$$f_a(x) := \begin{cases} \sin \frac{x + \pi}{2}, & -\pi \leq x < 0, \\ \sin \frac{3x - \pi}{2}, & 0 < x \leq \pi, \end{cases} \quad f_b(x) := \begin{cases} \cos \left(x - \frac{x}{2} \operatorname{sgn} \left(|x| - \frac{\pi}{2} \right) \right), & x < 0, \\ \cos \left(\frac{5}{2}x + x \operatorname{sgn} \left(|x| - \frac{\pi}{2} \right) \right), & x > 0, \end{cases}$$

and apply the concentration method to the Fourier partial sum, $\mathcal{I}_N(f)(x)$, to locate the edges of $f_a(x)$ and $f_b(x)$. Fig. 3 shows the detection of these jump discontinuities.

3.4. Enhancement of the concentration method

A method to improve the convergence property of the ‘concentration’ method was introduced in [9]. The results in (3.1) (and therefore (3.3)) are *enhanced* by amplifying the scales. Specifically, we start by amplifying the concentration property stated in Theorem 3.1. Thus, if $\{\alpha_j\}$ denote the location of the jump discontinuities and noting that $\sigma^r(1/N) \sim N^{-r}$, then (3.1) yields

$$(\tilde{S}_N^\sigma[f](x))^q \rightarrow \begin{cases} ([f](\alpha_j))^q & \text{if } x = \alpha_j, \\ (\log N/N)^q & \text{if } x \neq \alpha_j. \end{cases} \quad (3.4)$$

Next, we equilibrate: a more pronounced separation of scales is readily accomplished by defining

$$T := N^{q/2} (\tilde{S}_N^\sigma[f](x))^q \rightarrow \begin{cases} N^{q/2} ([f](\alpha_j))^q & \text{if } x = \alpha_j, \\ O(N^{-q/2}) & \text{if } x \neq \alpha_j. \end{cases} \quad (3.5)$$

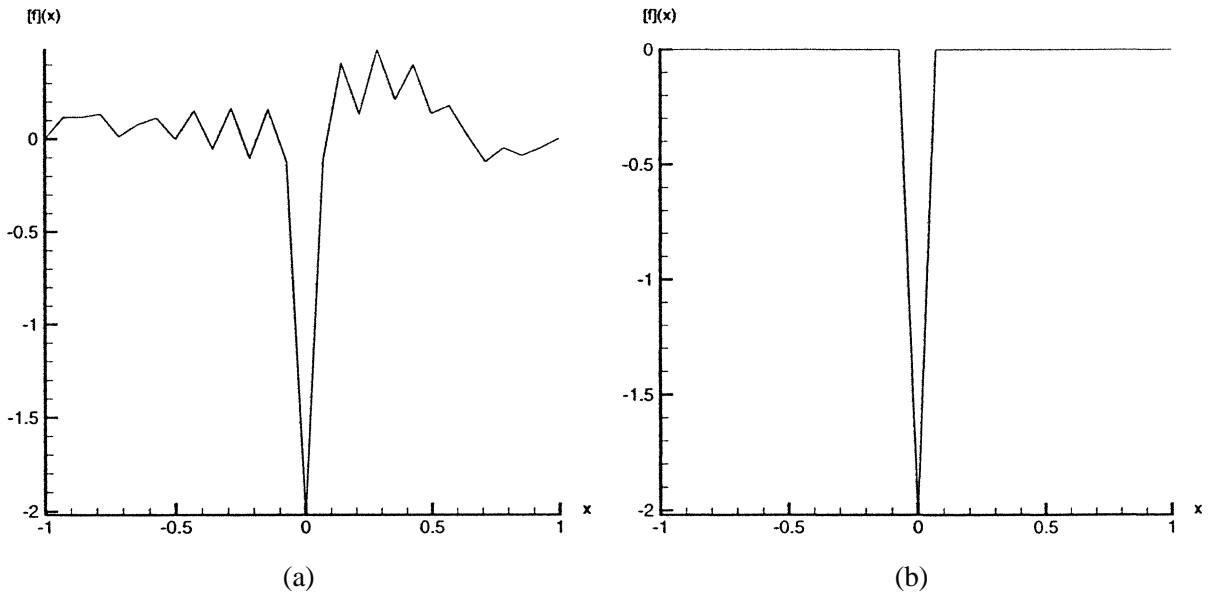


Fig. 4. Detection of discontinuous edges using the ‘concentrated’ Legendre partial sum $(\pi/N)\mathcal{I}'_N(f)(x)$ (a) and the enhancement (b) for the function $f_a(x)$ with $N = 40$.

The “enhanced” edge detection method is then computed as

$$\tilde{S}_N^e[f](x) = \begin{cases} \tilde{S}_N^\sigma[f](x) & \text{if } T > J_{\text{crit}}, \\ 0 & \text{if } T < J_{\text{crit}}. \end{cases} \quad (3.6)$$

Here J_{crit} is an $O(1)$ threshold parameter which signifies the critical (minimal) amplitude necessary for the jump discontinuities we would like to detect as admissible jumps—jumps with smaller amplitudes are ignored. The edges $x = \{\alpha_j\}_{j=1}^J$ are then simply determined as the locations corresponding to the nonzero values of (3.6). The separation of scales in (3.5) is the key to actually *pinpointing* the jump discontinuities, as shown in Figs. 4 and 5 for the Legendre pseudo-spectral case.

We emphasize that it is this enhancement of the concentration method that allows us to apply a post-processing method to the SV-solution, as explained in Section 4.

4. An effective post-processing method

Since the underlying exact solution, $f(x) = u(x, T)$, is only piecewise smooth, its spectral projections, $S_N[f](x)$, $\mathcal{I}_N[f](x)$, yield poor results. First order convergence is obtained away from the discontinuities and $O(1)$ spurious Gibbs oscillations are exhibited at the discontinuities. The removal of the Gibbs phenomenon has been the subject of several papers, e.g., [2,7,11,12]. Here we use the Gegenbauer post-processing method [12] which effectively eliminates the Gibbs’ phenomenon and recovers piecewise smooth functions with spectral accuracy in the maximum norm for each smooth interval *up to* the points of discontinuity.

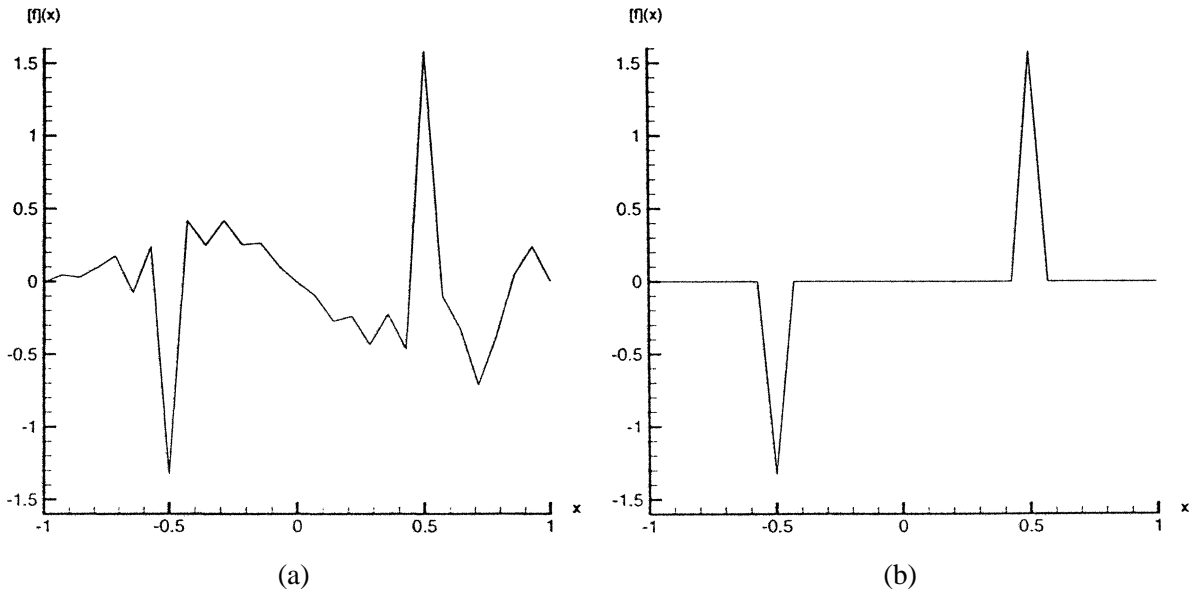


Fig. 5. Detection of discontinuous edges using the ‘concentrated’ Legendre partial sum $(\pi/N)\mathcal{I}'_N(f)(x)$ (a) and the enhancement (b) for the function $f_b(x)$ with $N = 40$.

4.1. The Gegenbauer post-processing method

Let us recall the Gegenbauer partial sum expansion for a smooth function $f(x)$, $x \in [-1, 1]$,

$$f_m(x) = \sum_{l=0}^m \widehat{f}_l^\lambda C_l^\lambda(x) \rightarrow f(x), \quad (4.1)$$

where \widehat{f}_l^λ are the Gegenbauer coefficients defined by

$$\widehat{f}_l^\lambda = \frac{1}{h_l^\lambda} \int_{-1}^1 (1-x^2)^{\lambda-1/2} C_l^\lambda(x) f(x) dx. \quad (4.2)$$

The Gegenbauer polynomials are orthogonal under the weight function $(1-x^2)^{\lambda-1/2}$ implying:

$$\int_{-1}^1 (1-x^2)^{\lambda-1/2} C_k^\lambda(x) C_n^\lambda(x) dx = \delta_{k,n} h_n^\lambda, \quad h_n^\lambda = \pi^{1/2} C_n^\lambda(1) \frac{\Gamma(\lambda+1/2)}{\Gamma(\lambda)(n+\lambda)}.$$

The Gegenbauer post-processing method requires two ingredients: (1) the (pseudo-)spectral approximation $S_N[f](x)$ and (2) the intervals of smoothness, $I_{j+1/2} = [\alpha_j, \alpha_{j+1}]$, as obtained in Section 3. The idea is to first approximate the Gegenbauer coefficients (4.2) from information extracted from $S_N[f](x)$, and then to use these approximated coefficients to construct the Gegenbauer partial sum expansion (4.1) in each smooth interval $I_{j+1/2}$. More specifically, the Gegenbauer coefficients \widehat{f}_l^λ are approximated for $x \in I_{j+1/2}$ by

$$\begin{aligned} \widehat{g}_l^\lambda &= \frac{1}{h_l^\lambda} \int_{-1}^1 (1 - \xi^2)^{\lambda-1/2} C_l^\lambda(\xi) S_N[f](x(\xi)) \, d\xi \\ &\sim \frac{\pi}{\mathcal{N}} \sum_{j=0}^{\mathcal{N}} \frac{C_l^\lambda(\xi_j) S_N[f](x(\xi_j)) (1 - \xi_j^2)^\lambda}{c_j}, \quad c_j = \begin{cases} 1 & \text{if } j = 1, \dots, \mathcal{N} - 1, \\ 2 & \text{if } j = 0, \mathcal{N}, \end{cases} \end{aligned} \tag{4.3}$$

where we have defined the local variable $\xi \in [-1, 1]$ with Gauss–Lobatto points ξ_j and \mathcal{N} as a constant large enough to satisfy the Gauss–Lobatto quadrature rule.

The coefficients \widehat{g}_l^λ are now used in the partial Gegenbauer sum to approximate the original function $f(x)$ as

$$g_m^\lambda(x(\xi)) = \sum_{l=0}^m \widehat{g}_l^\lambda C_l^\lambda(\xi). \tag{4.4}$$

It has been shown [12] that $g_m^\lambda(x(\xi))$ converges exponentially to $f(x)$ in the maximum norm provided the parameters $m, \lambda \sim N$.

4.2. Numerical examples

To illustrate the effectiveness of Gegenbauer post-processing, consider the two examples given in Section 3:

$$f_a(x) := \begin{cases} \sin \frac{x + \pi}{2}, & -\pi \leq x < 0, \\ \sin \frac{3x - \pi}{2}, & 0 < x \leq \pi, \end{cases} \quad f_b(x) := \begin{cases} \cos \left(x - \frac{x}{2} \operatorname{sgn} \left(|x| - \frac{\pi}{2} \right) \right), & x < 0, \\ \cos \left(\frac{5}{2}x + x \operatorname{sgn} \left(|x| - \frac{\pi}{2} \right) \right), & x > 0. \end{cases}$$

In both cases, information is extracted from the Fourier pseudo-spectral approximation $S_N[f](x)$ with the jump locations determined by the enhanced edge detection method in Section 3. The Gibbs phenomenon is clearly depicted in Fig. 6, where no post-processing has been used, while Fig. 7 shows the reconstruction of the piecewise smooth functions using the Gegenbauer post-processing method.

It is necessary to point out that in our case, the SV-solution $u_N(x, t)$ serves as highly accurate approximation of the exact projection, $u_N(x, T) \sim S_N[f](x)$. Only partial theoretical justifications in this direction can be found, e.g., [21,27]. Nevertheless, numerical results indicate that exponential accuracy can be achieved by applying the Gegenbauer post-processing method to the SV-solution $u_N(x, T)$ [22]. The same inference can be made for the shock location (edge detection) method in Section 3, i.e., the theoretical results are limited to locating the jump discontinuities of a piecewise smooth $f(x)$, but numerical evidence strongly advocates applying the enhanced edge detection method to the SV-solution $u_N(x, T)$.

5. The enhanced SV-method

Equipped with the results from the previous sections, we are now ready to implement a fully automated numerical method, the enhanced SV-method, that yields high accuracy to the conservation law (1.1) and

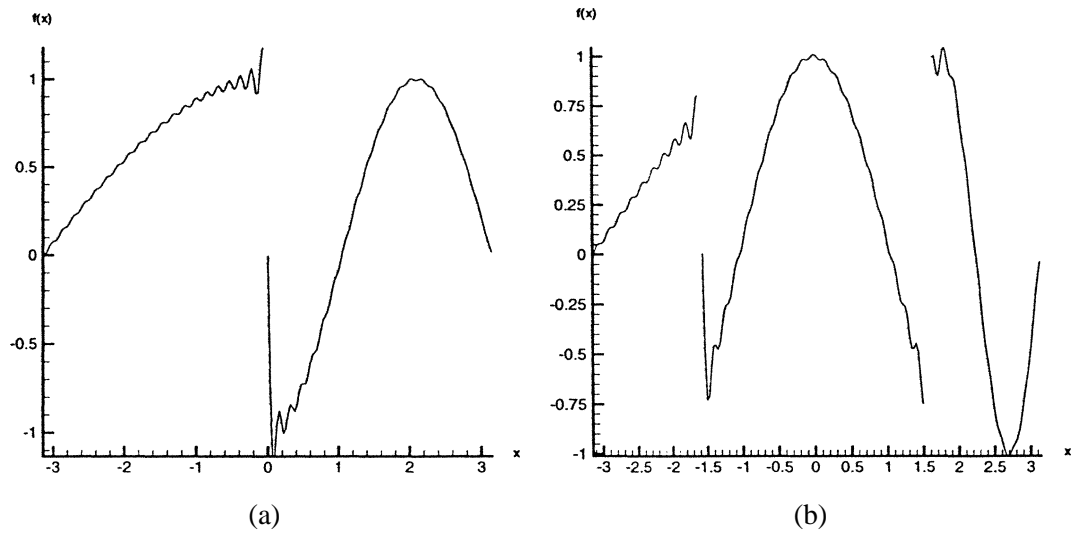


Fig. 6. Fourier partial sum, $S_{40}[f](x)$, of $f = f_a(x)$ (a) and $f = f_b(x)$ (b).

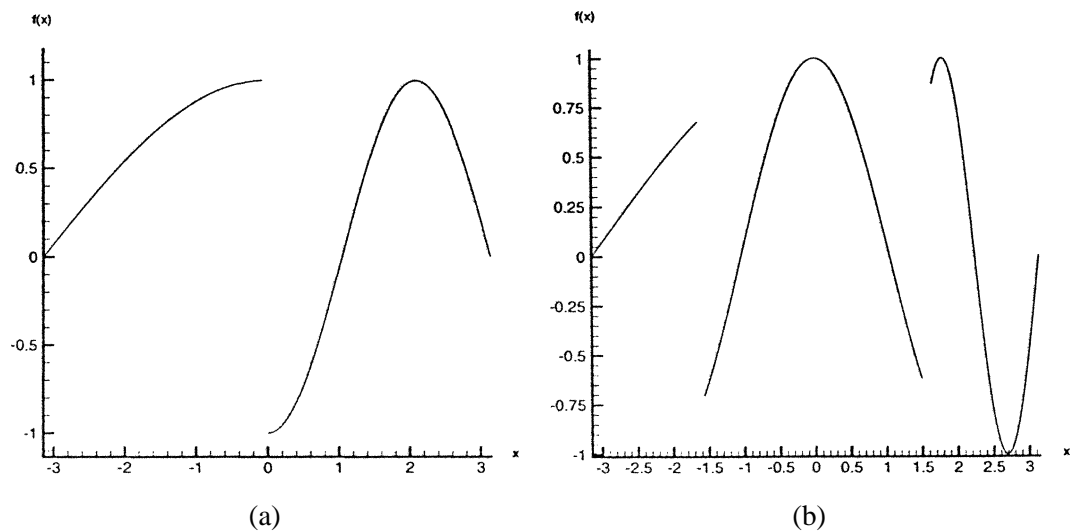


Fig. 7. Reconstruction of a piecewise continuous functions, $f = f_a(x)$ (a) and $f = f_b(x)$ (b), after post-processing with the Gegenbauer method.

strongly resolves the shock discontinuities. We emphasize that only the first step, the SV-approximation, is time-implemented. Subsequent steps are only performed once, at the final time T . The steps of the enhanced SV-method are:

1. Compute the SV-approximation $u_N(x, T) = u_N(x)$, $x \in [-1, 1]$.
2. Locate the shock discontinuities by employing the ‘concentration’ method

$$(-1)^p \frac{\pi(2p+1)}{N^{2p+1}} \frac{d^{2p+1}}{dx^{2p+1}} \mathcal{I}_N(u_N)(x),$$

where $\mathcal{I}_N(u_N)(x)$ is determined from the pseudo-spectral coefficients

$$\hat{u}_k = \sum_{j=0}^N u_N(x_j) L_k(x_j) \omega_k$$

with respect to the weight function ω_k and Lobatto collocation points x_j .

- Determine the intervals of smoothness $I_{j+1/2} = [\alpha_j, \alpha_{j+1}]$, $j = 0, \dots, J - 1$, $\alpha_0 = -1$ and $\alpha_J = 1$, from the ‘enhanced’ edge detection method (3.6)

$$\tilde{S}_N^e[u_N](x) = \begin{cases} \tilde{S}_N^\sigma[u_N](x) & \text{if } T > J_{\text{crit}}, \\ 0 & \text{if } T < J_{\text{crit}}. \end{cases}$$

This process can be employed repeatedly to find the discontinuities of $(d^l/dx^l)u_N(x)$ and to determine intervals of C^l -smoothness $I_{j_l+1/2}^l = [\alpha_{j_l}^l, \alpha_{j_l+1}^l]$, $j_l = 0, \dots, J_l - 1$, with $\alpha_0^l = -1$ and $\alpha_{J_l}^l = 1$. More specifically:

- After the shock locations $x = \{\alpha_j\}_{j=0}^{J-1}$ are determined, $u_N(x)$ is differentiated in each C^0 -smooth interval $I_{j+1/2}$. The concentration method and enhanced edge detection method are performed in each C^0 -smooth interval to locate the discontinuities $x = \{\beta_k\}_{k=0}^{K-1}$ of $(d/dx)\mathcal{I}_N(u_N)(x)$.
 - The shock locations $\{\alpha_j\}_{j=0}^{J-1}$ and the contact discontinuity locations $\{\beta_k\}_{k=0}^{K-1}$ are arranged in increasing order to form $\{\alpha_{j_1}^1\}_{j_1=0}^{J_1-1}$, $J_1 = K + J$ to determine each C^1 -smooth interval $I_{j_1+1/2}^1 = [\alpha_{j_1}^1, \alpha_{j_1+1}^1]$.
 - This process is repeated to obtain the C^l -smooth intervals $I_{j_l+1/2}^l = [\alpha_{j_l}^l, \alpha_{j_l+1}^l]$.
- Approximate the Gegenbauer coefficients inside each interval $I_{j_l+1/2}^l$:

$$\hat{g}_\mu^\lambda = \frac{\pi}{\mathcal{N}} \sum_{j=0}^{\mathcal{N}} \frac{C_\mu^\lambda(\xi_j) S_N[f](x(\xi_j)) (1 - \xi_j^2)^\lambda}{c_j}, \quad c_j = \begin{cases} 1 & \text{if } j = 1, \dots, \mathcal{N} - 1, \\ 2 & \text{if } j = 0, \mathcal{N}. \end{cases}$$

- Use these coefficients to apply the Gegenbauer reconstruction method in each interval $I_{j_l+1/2}^l$:

$$g_m^\lambda(x(\xi)) = \sum_{\mu=0}^m \hat{g}_\mu^\lambda C_\mu^\lambda(\xi) \rightarrow u(x).$$

6. Numerical examples

Presented here are numerical simulations of the enhanced SV-method to the scalar periodic inviscid Burgers’ equation, and to the Euler equations of gas dynamics. The parameters for the periodic and non-periodic SV-method, ε_N and m_N , were taken, respectively, as in [18,24]. Although the parameters for the Gegenbauer reconstruction were not formally optimized, an effort was made to obtain the best overall accuracy. For the inviscid Burgers’ equation the best numerical results were achieved using $\lambda = 1$ and $m = 3$ for each piecewise smooth subinterval, although similar results were obtained using any $\lambda \in [1, 8]$. We used $\lambda = 1$ and $m = 3$ for each variable in the Euler equations.

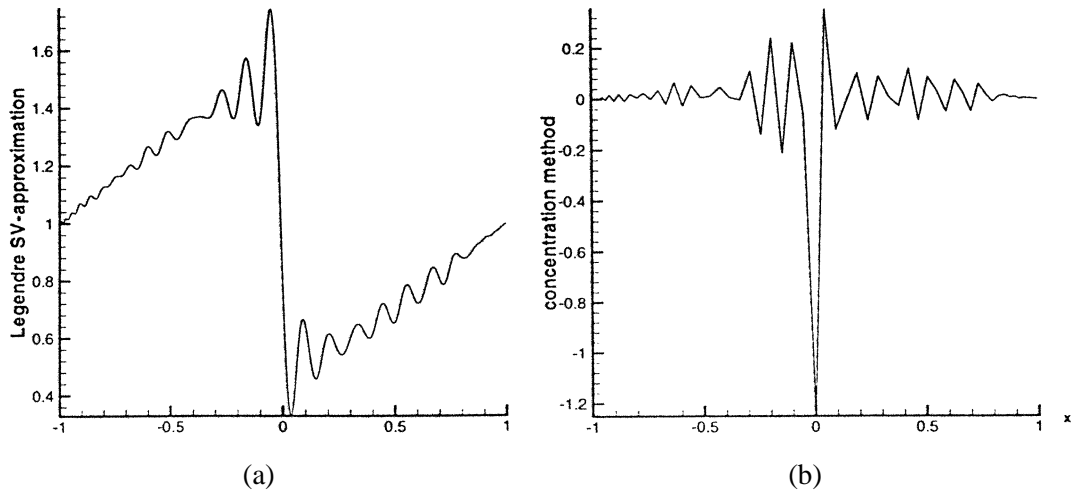


Fig. 8. (a) The solution to the inviscid Burgers' equation with periodic boundary conditions at time $T = 1$ using the Legendre SV-approximation with $N = 64$. (b) Edge detection using the Legendre concentration method.

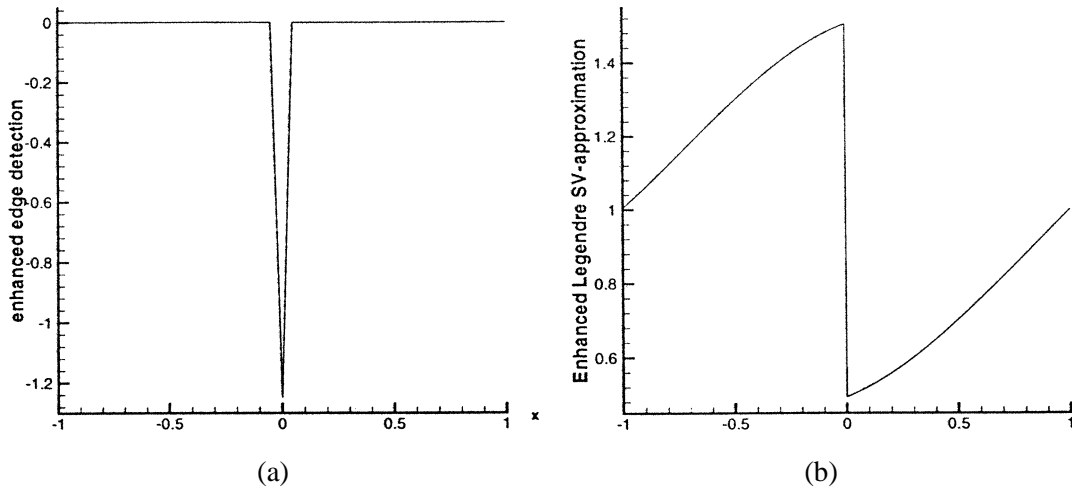


Fig. 9. (a) The application of the enhanced edge detection to the results in Fig. 8. (b) The numerical solution to the inviscid Burgers' equation using the enhanced SV-approximation method.

Example 6.1 (Periodic inviscid Burgers' equation).

$$\frac{\partial}{\partial t} u(x, t) + \frac{\partial}{\partial x} \left(\frac{u^2(x, t)}{2} \right) = 0.$$

1. For the enhanced Fourier SV-method: $(x, t) \in [-\pi, \pi] \times [0, \infty)$, with the initial conditions $u(x, 0) = \sin x$, and the prescribed boundary conditions, $u(-\pi, t) = u(\pi, t)$.
2. For the enhanced Legendre SV-method: $(x, t) \in [-1, 1] \times [0, \infty)$, with the initial conditions $u(x, 0) = \frac{1}{2} \sin \pi x + 1$ and the prescribed boundary conditions $u(-1, t) = g(t)$ (where $g(t) := u(1, t)$).

Table 1

Maximum errors for the periodic scalar inviscid Burgers' equation using both the Fourier and Legendre enhanced SV-methods for $N = 8, 16, 32, 64$

N	8	16	32	64
Fourier	0.260	0.148	6.5E-02	1.1E-02
Legendre	0.118	6.2E-02	3.7E-02	6.5E-03

Figs. 8 and 9 show the results for the regular Legendre SV-method and the enhanced Legendre SV-method for the periodic inviscid Burgers' equation. In particular, we quote in Table 1 the *maximum* errors as an indication to the high-resolution of the enhanced SV results.

Next, we turn to demonstrate the performance of the enhanced Legendre SV-method for one-dimensional system of Euler equations of gas dynamics. In this example we must use the enhanced edge detection procedure to locate the discontinuities in the first derivative as well. This allows us to obtain very high resolution and eliminate the “smearing” effect of the post-processing method caused by the contact discontinuities.

Example 6.2 (Euler equations of gas dynamics).

$$\frac{\partial}{\partial t} u(x, t) + \frac{\partial}{\partial x} f(u(x, t)) = 0, \quad u = \begin{bmatrix} \rho \\ \rho v \\ E \end{bmatrix}, \quad f(u) = \begin{bmatrix} \rho v \\ \rho v^2 + p \\ v(E + p) \end{bmatrix},$$

where ρ denotes the density of the gas, $m = \rho v$ its momentum, E its energy per unit volume and $p = (\gamma - 1) \cdot (E - \frac{1}{2}\rho v^2)$ its (polytropic) pressure, $\gamma = 1.4$. The Riemann shock tube problem [23] has initial conditions

$$u(x, 0) = \begin{cases} u_l = (1.0, 0.0, 2.5)^T, & x < 0, \\ u_r = (0.125, 0.0, 0.25)^T, & x > 0. \end{cases}$$

Example 6.2 is simulated by the enhanced Legendre SV-method and the Adam–Bashforth timestepping with $N = 128$ and $\Delta t = 10^{-5}$. Fig. 10 shows how the enhanced edge detection method locates the shock discontinuities for density, ρ , in Example 6.2, while Fig. 11 displays the location of contact discontinuities. We observe the high resolution attained by the enhanced SV-method; this high-resolution could not be realized without the enhanced edge detection of Section 3.4.

The profiles for the enhanced Legendre SV-solutions of density (ρ), velocity (v), and pressure (p) are shown in Figs. 12–14.

7. Conclusion

The enhanced SV-method provides a stable and accurate way to approximate a broad class of one-dimensional conservation laws. The key to the improvement of the enhanced SV-method over the original SV-method [18,24] is the enhanced edge detection method [9] which “pinpoints” the shock

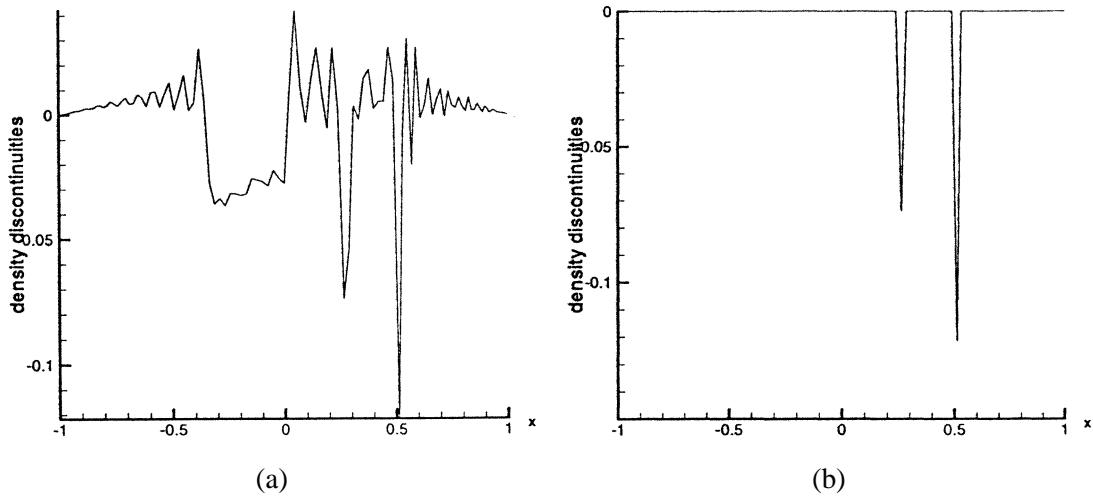


Fig. 10. Detection of the shock discontinuities using the ‘concentrated’ method (a) and the enhanced edge detection method (b).

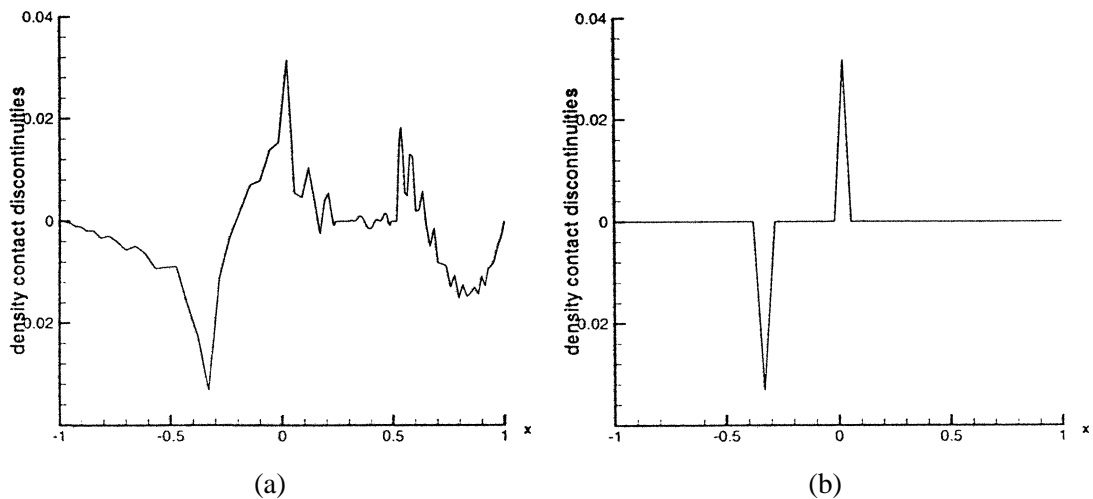


Fig. 11. Detection of the contact discontinuities using the ‘concentrated’ method (a) and the enhanced edge detection method (b).

discontinuities formed by the nonlinear conservation laws. Since the SV-approximation retains enough information, the enhanced edge detection and post-processing methods must be performed only once at the final time step, adding minimal cost to the original SV-method. Although there is no formal proof of spectral accuracy, the numerical experiments strongly indicate that high accuracy and high resolution at the shock discontinuities are both attainable. We emphasize that the enhanced SV-approximation for one-dimensional systems is a simple, fully automated, and comprehensive method that requires no solving of Riemann invariants. Some remarks are in order:

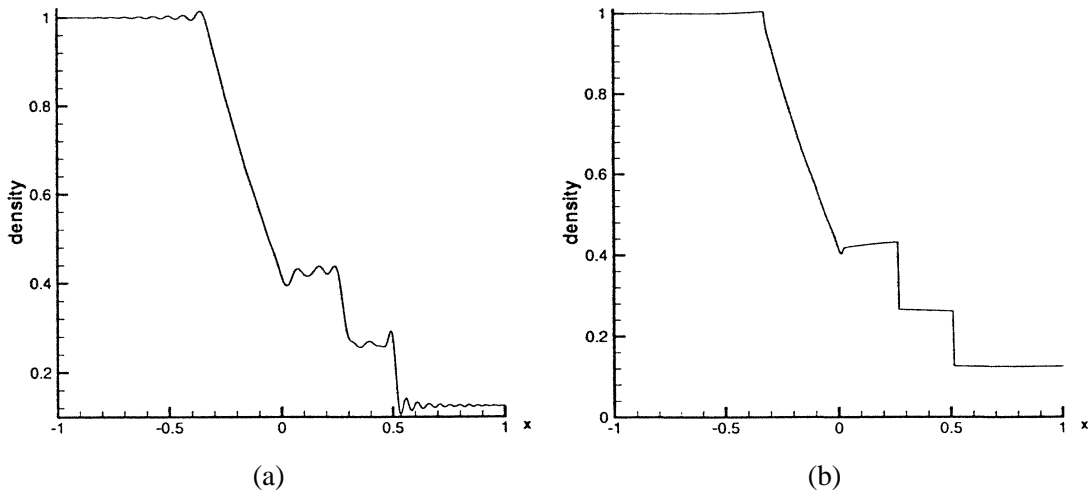


Fig. 12. Density profile using the Legendre SV-method (a) and the enhanced version (b).

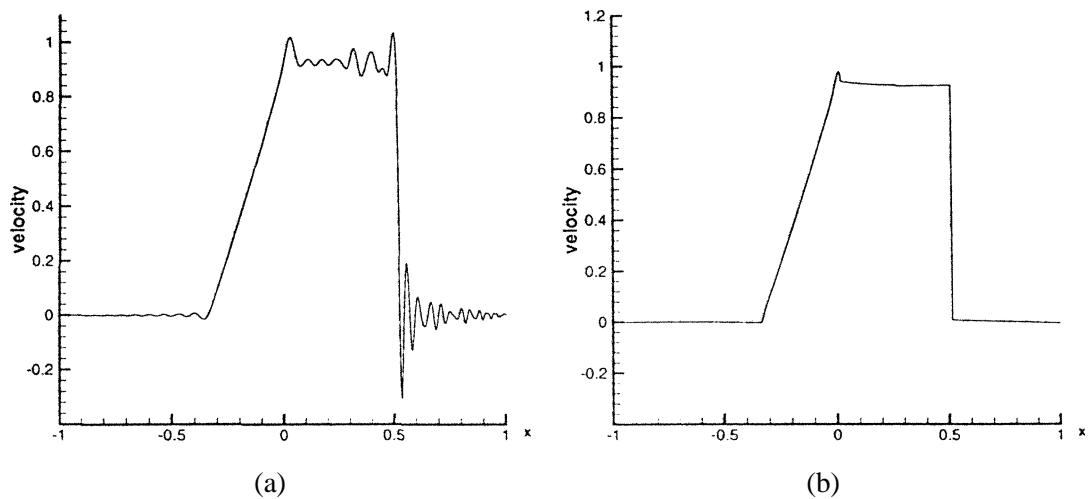


Fig. 13. Velocity profile using the Legendre SV-method (a) and the enhanced version (b).

1. *Efficiency.* A fast Legendre transform is available [6], improving the speed of the Legendre SV-method considerably.
2. *Time discretization.* A fourth order Runge–Kutta scheme was implemented as well as the Adam–Bashforth method but did not alter the final results.
3. *Spectral accuracy.* The theoretical justification for applying the Gegenbauer post-processing solution to the SV-approximation remains an open question. Such justification may prove that the results of the enhanced SV-method are in fact exponentially accurate. In this context, we refer to [26], and in particular the recent approach presented in [28], for pointwise error estimates of piecewise-smooth solutions.

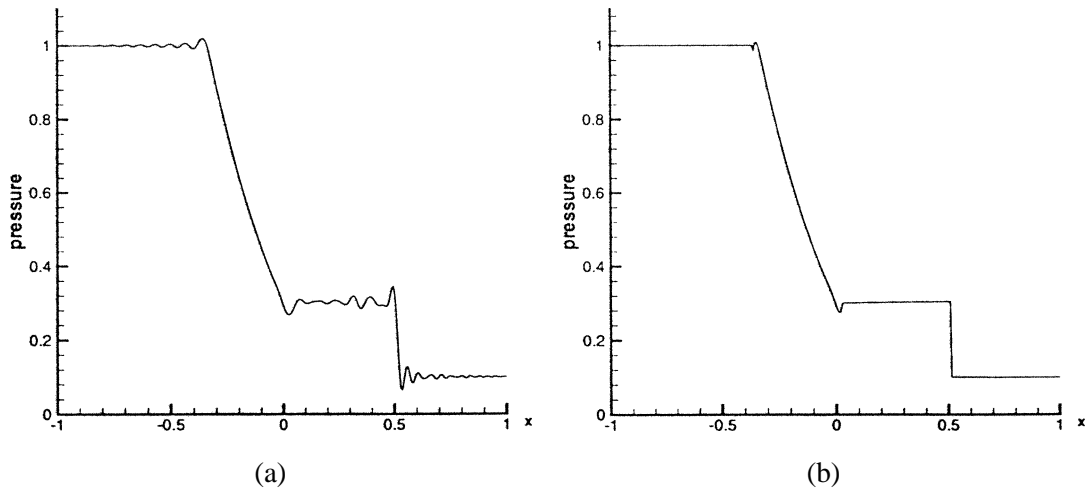


Fig. 14. Pressure profile using the Legendre SV-method (a) and the enhanced version (b).

4. *Contact discontinuities.* The resolution of the contact discontinuity—a particularly difficult linear-like field to be detected by high-resolution finite-difference schemes, is detected here by the density field. Its recovery without spurious oscillations in the pressure field is particularly impressive.
5. *High-resolution and optimal parameterization.* Although the figures presented clearly demonstrate the high resolution content of the enhanced SV method, there are still spurious spikes which could be noticed, particularly at the tips of the rarefactions. Also, we should emphasize that we have *not* optimized the various parameters, particularly those parameters involved in the Gegenbauer reconstruction. Such optimization could have further improved the results of the less accurate density field, for example. These as well as other improvements are left for future work.

References

- [1] Ø. Andreassen, I. Lie, C.E. Wasberg, The spectral viscosity method applied to simulation of waves in a stratified atmosphere, *J. Comput. Phys.* 110 (1994) 257–273.
- [2] N.S. Banerjee, J. Geer, Exponentially accurate approximations to piecewise smooth periodic functions, ICASE Report No. 95-17, NASA Langley Research Center, 1995.
- [3] N. Bary, *Treatise of Trigonometric Series*, The Macmillan Company, New York, 1964.
- [4] H.S. Carslaw, *Introduction to the Theory of Fourier's Series and Integrals*, Dover, 1950.
- [5] G.-Q. Chen, Q. Du, E. Tadmor, Spectral viscosity approximations to multidimensional scalar conservation laws, *Math. Comp.* 61 (1993) 629–643.
- [6] W.S. Don, A. Solomonoff, *Pseudopack*, Division of Applied Mathematics, Brown University, 1996.
- [7] K.S. Eckhoff, Accurate reconstructions of functions of finite regularity from truncated series expansions, *Math. Comp.* 64 (1995) 671–690.
- [8] A. Gelb, E. Tadmor, Detection of edges in spectral data, *Appl. Comp. Harmonic Anal.* 7 (1999) 101–135.
- [9] A. Gelb, E. Tadmor, Detection of edges in spectral data II. Nonlinear enhancement, Preprint, UCLA CAM Report No. 99-23.
- [10] B.I. Golubov, Determination of the jump of a function of bounded p -variation by its Fourier series, *Math. Notes* 12 (1972) 444–449.

- [11] D. Gottlieb, E. Tadmor, Recovering Pointwise Values of Discontinuous Data within Spectral Accuracy, in: E.M. Murman, S.S. Abarbanel (Eds.), *Progress and Supercomputing in Computational Fluid Dynamics, Proceedings of a 1984 U.S.–Israel Workshop, Progress in Scientific Computing, Vol. 6*, Birkhäuser, Boston, 1985, pp. 357–375.
- [12] D. Gottlieb, C.-W. Shu, On the Gibbs phenomenon and its resolution, *SIAM Rev.* 39 (1998) 644–668.
- [13] D. Gottlieb, C.-W. Shu, A. Solomonoff, H. Vandeven, On the Gibbs phenomenon I: recovering exponential accuracy from the Fourier partial sum of a nonperiodic analytic function, *J. Comput. Appl. Math.* 43 (1992) 81–92.
- [14] G. Kvernadze, Determination of the jump of a bounded function by its Fourier series, *J. Approx. Theory* 92 (1998) 167–190.
- [15] P.D. Lax, *Hyperbolic Systems of Conservation Laws and the Mathematical Theory of Shock Waves*, CBMS-NSF Regional Conference Series in Applied Mathematics, Vol. 11, SIAM, Philadelphia, PA, 1972.
- [16] H. Ma, Chebyshev–Legendre spectral viscosity method for nonlinear conservation laws, *SIAM J. Numer. Anal.* 35 (1998) 869–892.
- [17] H. Ma, Chebyshev–Legendre super spectral viscosity method for nonlinear conservation laws, *SIAM J. Numer. Anal.* 35 (1998) 893–908.
- [18] Y. Maday, S.M. Ould Kaber, E. Tadmor, Legendre pseudospectral viscosity method for nonlinear conservation laws, *SIAM J. Numer. Anal.* 30 (1993) 321–342.
- [19] A. Majda, J. McDonough, S. Osher, The Fourier method for nonsmooth initial data, *Math. Comp.* 30 (1978) 1041–1081.
- [20] S.M. Ould Kaber, A Legendre pseudospectral viscosity method, *J. Comput. Phys.* 128 (1996) 165–180.
- [21] S. Schochet, The rate of convergence of spectral viscosity methods for periodic scalar conservation laws, *SINUM* 27 (1990) 1142–1159.
- [22] C.W. Shu, P. Wong, A note on the accuracy of spectral method applied to nonlinear conservation laws, *J. Sci. Comput.* 10 (1995) 357–369.
- [23] J. Smoller, *Shock Waves and Reaction–Diffusion Equations*, Springer-Verlag, New York, 1983.
- [24] E. Tadmor, Convergence of spectral methods for nonlinear conservation laws, *SIAM J. Numer. Anal.* 26 (1989) 30–44.
- [25] E. Tadmor, Shock capturing by the spectral viscosity method, *Comput. Methods Appl. Mech. Engrg.* 80 (1990) 197–208.
- [26] E. Tadmor, Total-variation and error estimates for spectral viscosity approximations, *Math. Comp.* 60 (1993) 245–256.
- [27] E. Tadmor, Super viscosity and spectral approximations on nonlinear conservation laws, in: M.J. Baines, K.W. Morton (Eds.), *Numerical Methods for Fluid Dynamics IV, Proceedings of the 1992 Conference on Numerical Methods for Fluid Dynamics*, Clarendon Press, Oxford, 1993, pp. 69–82.
- [28] E. Tadmor, T. Tang, Pointwise error estimates for scalar conservation laws with piecewise smooth solutions, *SIAM J. Numer. Anal.*
- [29] J. Von Neumann, R.D. Richtmyer, A method for the numerical calculations of hydrodynamical shocks, *J. Appl. Phys.* 21 (1950) 232–237.
- [30] A. Zygmund, *Trigonometric Series*, Cambridge University Press, 1959.